DEEP HST-WFPC2 PHOTOMETRY OF NGC 288. II. THE MAIN SEQUENCE LUMINOSITY FUNCTION [1]

Michele Bellazzini, Flavio Fusi Pecci[1], Paolo Montegriffo, Maria Messineo[2]
INAF - Osservatorio Astronomico di Bologna, Via Ranzani 1, 40127, Bologna, ITALY
bellazzini@bo.astro.it, flavio@bo.astro.it, messineo@strw.leidenuniv.nl
Lorenzo Monaco
Dip. di Astronomia, Università di Bologna, Via Ranzani 1, 40127, Bologna, ITALY
s_monaco@bo.astro.it
AND
Robert T. Rood
Department of Astronomy, University of Virginia, P.O. Box 3818, Charlottesville, VA, 22903-0818
rtr@virginia.edu
Accepted by AJ - BAP02-2002-04-OAB

ABSTRACT

The Main Sequence Luminosity Function (LF) of the Galactic globular cluster NGC 288 has been obtained using deep WFPC2 photometry. We have employed a new method to correct for completeness and fully account for bin-to-bin migration due to blending and/or observational scatter. The effect of the presence of binary systems in the final LF is quantified and is found to be negligible. There is a strong indication of the mass segregation of unevolved single stars and clear signs of a depletion of low mass stars in NGC 288 with respect to other clusters. The results are in good agreement with the prediction of theoretical models of the dynamical evolution of NGC 288 that take into account the extreme orbital properties of this cluster.

Subject headings: clusters: globular clusters: individual (NGC 288) - luminosity function

1. INTRODUCTION

After a decade of HST observations, the Luminosity Function (LF) of unevolved Main Sequence (MS) stars has been derived for several Galactic globular clusters (GGCs). In many cases the LF extends down to the faintest stellar objects ($M \simeq 0.1\,M_{\odot}$; see, e.g., King et al. 1998; Bedin et al. 2001). For unevolved stars, the luminosity directly tracks the mass, the most fundamental parameter of a star. The determination of the Initial Mass Function (IMF) from the observed LF of Main Sequence stars, as well as the study of the of the variation of the LF within a given cluster and among different clusters is now a well established field of research which has provided important insights on the dynamical evolution of GCCs (see, e.g., Ferraro et al. 1997; King et al. 1998; Marconi et al. 1998; Piotto & Zoccali 2000; Paresce & De Marchi 2000, and references therein). In particular, the signature of mass segregation, due to the energy equipartition established by two body encounters among clusters stars, has been detected in many clusters by comparing the LFs obtained at different distances from the cluster center. Also, the effect of the pruning of the outer extremities of the clusters by the Galactic tidal field or by the violent interaction with the Galactic bulge and disc have been shown with the analysis of the LF of MS stars (see, e.g., Andreuzzi et al. 2001, and references therein).

Here we present the MS LF of the globular cluster NGC 288 down to $V \sim 24.5$. The LF was based on HST-WFPC2 observations that are described in detail in a companion paper (Bellazzini et al. 2001b, hereafter Pap I), that was devoted to the study of the binary population of this cluster. In Pap I we used a method very similar to the one adopted by Rubenstein & Bailyn (1997), based on extensive sets of artificial star experiments, to estimate the global binary fraction (f_b) of the cluster ($7\ \% \leq f_b \leq 30\ \%$) and to show that binary systems are spatially segregated within the cluster. These same artificial star experiments can be used to obtain LFs in different regions of the cluster, *corrected for all observational effects*. In §2 we will briefly recall the characteristics of the adopted sample and of the artificial star experiments, as well as the results of Pap I that are relevant in the present context. In §3 we introduce a *new method* to correct the observed LF. The effect of the presence of binary systems on the final LF is also discussed and quantified with the support of the analysis performed in Pap I. In §4 we present the final LF of NGC 288 and compare it with the LFs of other clusters and, finally, in §5 we summarize our results.

1.1. *The globular cluster NGC 288*

NGC 288 is a loose ($\log \rho_0 = 1.80\ L_{\odot V}\, pc^{-3}$; Djorgovski 1993) cluster. It is a classical old GGC (Rosenberg et al. 1999) with a blue Horizontal Branch (HB) morphology (see Bellazzini et al. 2001a; Catelan et al. 2001, and references therein). Its stars are not exceedingly metal deficient ([Fe/H] $= -1.39$) and have the abundance pattern typical of halo stars (Shetrone & Keane 2000). The cluster lies on a very inclined and eccentric orbit that carries it into the inner, denser region of the Galaxy, where the effects of Galactic tides and disc/bulge shocks are more disruptive

[1] INAF - Stazione Astronomica di Cagliari, Loc. Poggio dei Pini, Strada 54, 09012 Capoterra (CA), ITALY
[2] presently at Sterrenwach Leiden, Postbus 9513, 2300 RA Leiden, The Netherlands

. According to Dinescu, Girard & van Altena (1999) the perigalactic distance is $R_p \simeq 1.8$ kpc, the eccentricity is $e \simeq 0.7$, the orbital period is $P \simeq 220 \times 10^6$ years, and the "destruction rate" is one of the highest in the GGC system. The observed distance from the Galactic Center (Harris 1996, $R_{GC} \simeq 11$ kpc;) indicates that the cluster is presently near the apogalactic point of its orbit (see also Pasquali, Brigas & De Marchi 2000).

2. THE DATASET AND THE ARTIFICIAL STAR EXPERIMENT

The observations, the data reduction process and the artificial star experiments are described in detail in Pap I. Here we summarize the points that are relevant in the present context.

2.1. *The sample*

Two HST-WFPC2 fields were observed in the F555W and F814W passbands: one with the PC camera nearly centered on the center of the cluster (Int field), and one with the WF4 camera partially overlapping the WF3-Int field (Ext field; see Fig. 1 of Pap I). The Int field is almost completely enclosed in the region within 1 half light radius ($1\,r_h \simeq 1.6\,r_c$; where $r_c = 85''$ is the core radius) Djorgovski 1993) while the Ext field samples a region contained in the annulus $1\,r_h < r < 2\,r_h$, where r is the distance from the cluster center. The data were transformed to the standard Johnson-Kron-Cousins photometric system by calibration to the ground-based data of Rosenberg et al. (2000). The Int sample contains 5766 sources from $V \sim 13$ to $V \sim 25$ and the Ext one contains 2013 sources between $V \sim 16$ and $V \sim 25.5$. The large majority of the observed stars are fainter than the Turn Off (TO) point ($V \simeq 19$), and hence are unevolved MS stars (and/or binary systems containing *two* unevolved MS stars; see Pap I). The F336W and F225W observations of the Int field that has been shortly discussed in Pap I are not used in the present paper.

2.2. *The artificial star experiments*

Simulations containing more than 80,000 artificial stars per chip have been made on the V, I frames. In each run of the artificial stars experiments $\simeq 100$ artificial stars per chip were added at the same position in the median image (that we used as a master-frame to obtain a list of positions of *bona fide stars*; see Pap I) and in each of the single frames (that were used to obtain accurate photometry; see Pap I). The set of experiments for a given chip (sub-field) was completed with ~ 800 independent runs. The final total number of artificial star experiments is $> 1,500,000$. For each artificial star a random input V magnitude is drawn from a distribution similar to the observed LF extrapolated to magnitudes slightly below the observed lower limit. This fainter limit was required so that the simulations would contain a large number of stars fainter than the observed limiting magnitude to correctly sample the magnitude bins where the incompleteness is expected to be highest (see Pap I).

We ultimately derive the true LF in a way that does not depend on the assumed artificial star LF (see §3.2). The input I is obtained from the input V using the cluster ridge line. Each simulated star thus had the appropriate color and was simultaneously added to the corresponding V and I frames at the same position. The simulated stars were randomly distributed on the frames with an additional constraint (see Pap I and also Tosi et al. 2001, for a detailed description of the method) preventing any interference between simulated stars. In practice, for each run of the artificial stars experiment, only one artificial star is added in each 80×80 pixel portion of a chip. The whole process of data reduction has been repeated on all the frames with artificial stars added and the *output* magnitudes have been recorded (see Pap I, for details).

Fig. 1 shows the *input* and *output* CMDs for the stars simulated in the PC-Int, PC-Ext, WF2-int and WF2-Ext frames. The WF2 samples have been chosen as representative of the WF cameras for the Int and Ext fields. Within a given field (Int and Ext) the observations with the different WF cameras have very similar properties (see Pap I). Note the different response to the same input color-magnitude distribution in the four cases represented. This arises because the larger pixels of the WF cameras allow them to reach fainter limiting magnitudes than the PC camera and because the Int and Ext fields have different average degrees of crowding.

All of the effects of the whole process of *observation and data reduction* on a large sample of stars representing a pure Simple Stellar Population (SSP) are shown in Fig. 1. These effects can be imagined to be the results of the application of a multi-dimensional function (that we will call Observation/Measure Function; hereafter OMF) on the *true* stars of the clusters, here represented by the input artificial stars lying on the ridge-line. In Pap I the empirical knowledge of the effects of the OMF has been used to extract the *signal* provided by the presence of a significant population of binary systems in the color distribution around the ridge-line from the observational noise due to random scatter, blending, etc. Here we will use it to correct the observed LF from all the spurious deformations due to the same factors.

2.3. *Completeness and division in subsamples*

The artificial star experiments have been carried out independently for each camera of each observed field. The completeness functions for each camera have been presented in Fig. 5 of Pap I. The crowding conditions of the dataset are never particularly critical, and the completeness is rather similar everywhere. The completeness factor (C_f) is larger than 80 % for $V \leq 23.5$ in all the samples except the PC-Int, the innermost one, where $C_f \geq 80$ % for $V \leq 22$. It has been shown that the spatial variation of completeness within a single camera are negligible. For the present purpose, we take advantage of the great similarity of crowding conditions in the WF cameras of the Int and Ext samples to subdivide the total sample in the following subsamples: (1) PC-Int, (2) WF-Int, containing the WF2-Int, WF3-Int and WF4-Int samples, (3) PC-Ext and, (4) WF-Ext, containing the WF2-Ext, WF3-Ext and WF4-Ext samples. The four subsamples are internally very homogeneous and cover different radial regions of the cluster. In this sense, the difference between the PC-Ext and the WF-Ext samples is small but we prefered to keep them separate because of the different limiting magnitude.

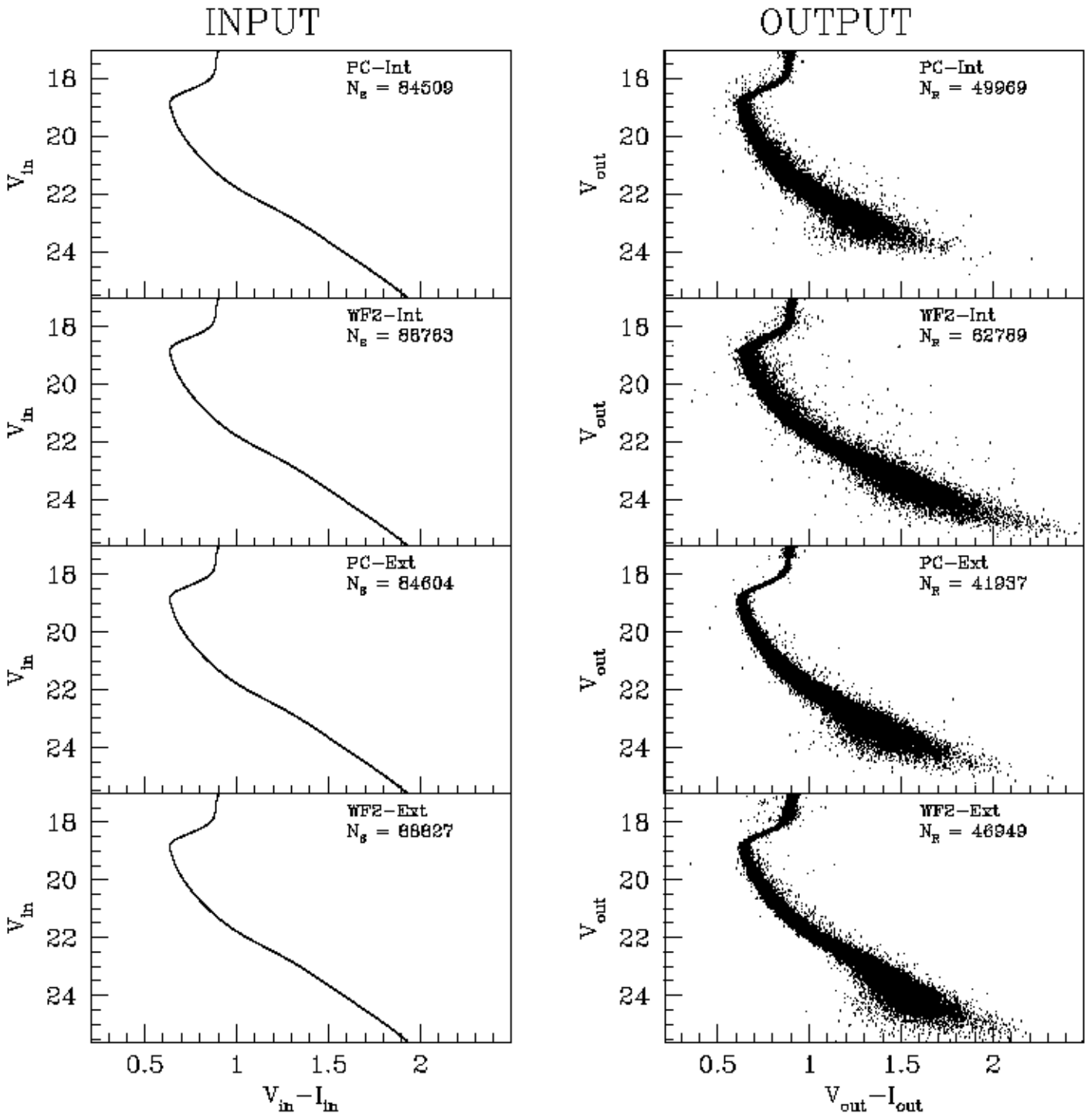

FIG. 1.— CMDs of the simulated stars obtained with the *input* magnitudes ($V_{\rm in}, I_{\rm in}$; left panels), and with the *output* magnitudes ($V_{\rm out}, I_{\rm out}$; right panels). The plot shows the effect of the observation - reduction process on the PC-Int and PC-Ext frames, while WF2-Int and WF2-Ext are shown as representative of the WF cameras in the Int and Ext samples, respectively. N_S is the total number of *simulated* stars while N_R is the total number of *recovered* stars. Note that the ratio between this two numbers is not directly comparable, at face value, since the limiting magnitude of the LF from which the artificial stars were drawn was different in the different cases. Since the observed limiting magnitude was different in the various cases, the limiting magnitude of the artficial stars LF was varied accordingly to exclude unnecessarily faint stars (e.g. more than ~ 1 mag below than the observed limiting magnitude) from the simulations.

3. THE CORRECTION OF THE OBSERVED LF

The effects of the OMF on the *true* properties of stars that may affect the LF derived from an observed sample are:

1. **Star loss.** Stars may be lost in the observation/measure process. This occurs for two different reasons:
   (a) Near the limiting magnitude of the observations a star can be succesfully detected if it falls on a positive fluctuation of the background that brings it *above* the detection threshold and can be *lost* if it falls on a *negative* fluctuation. This effect is purely stochastic; it does not depend on the crowding. It just depends on the amplitude of the random fluctuations of the background. There is a level of magnitude beyond which no possible positive fluctuation can bring a star above the detection threshold. All the stars fainter than this limit are lost (unobserved) and just contribute to the diffuse luminosity of the unresolved background.
   (b) Stars may be lost if they fall on a brighter source (star or galaxy) and/or if their images are badly corrupted by defects of the chip or the hit of a cosmic ray (this two latter effects are expected to have a negligible impact in the present case because of the adopted observation + data reduction strategy; see Pap I). This effect depends on the local degree of crowding as well as on the magnitude of the star.
2. **Blending.** A star may be blended with a fainter source and its measured magnitude will be brighter than the *true* one because of the flux contributed by the fainter blended source. Considered from the perspective of artificial stars experiments the maximum possible effect of a blending is to change the observed magnitude of a star by $\simeq 0.75$ mag. In fact, if we recover an artificial star by its (known) position in a frame with an output magnitude more than 0.75 mag brighter than its input magnitude, this means that it is fallen on a real star brighter than the simulated star. Thus, we are not recovering/measuring the simulated star but the real one instead, i.e., thus the artificial star has been lost.
3. **Observational scatter.** The magnitude of the *true* star is altered by all the sources of stocastic noise associated with the process of observation/data reduction (e.g., photon noise, imperfect PSF fit, etc.). The maximum possible effect of this factor is magnitude dependent and may be roughly evaluated on the basis of the typical error on a given measure. For instance, in the present case we included in the final samples only the stars with errors[4] lower than 0.2 mag in both I and V. Hence a $\sim 3\sigma$ fluctuation can change the magnitude of an observed star by ~ 0.6 mag, at most, near the limiting magnitude level.

The derived LFs are in practice histograms of the number of stars as a function of magnitude. The factors above change the *true* LF histogram by depopulating the bins as a function of (increasing) magnitude (mainly factor 1) and by moving stars from one bin to another (migration) due to the magnitude changes induced by factor 2 and/or 3. However factors 2 and 3 are strictly interwoven and their effect cannot be separated. For example, a given star may be moved, say, 0.4 mag brighter because it is blended with a fainter unresolved source, but it might simultaneously be affected by a negative fluctuation of the random observational scatter, so its final magnitude may differ from the true one by just 0.2 mag. A blending between two unresolved sources can bring them above the detection threshold, injecting in the sample two stars that should have been lost if not blended[5]. The possibilities are too numerous to list here. The real contribution of the three effects cannot be known for a the specific case. On the other hand, it is clear that we can obtain a statistical knowledge of the actual LF.

The traditional way to recover the *true* LF from an observed one consists in multiplying the numbers in each bin of the observed LF by the inverse of the Completeness factor ($C_f = N_R/N_S$; where N_R is the number of *recovered* stars and N_S is the number of the *simulated* ones) at the center of the bins. It is clear that such procedure corrects at first order only for the effects of star loss (factor 1) while the effects of the other factors are ignored. A popular misconception is that the observational scatter cannot produce bin migration if the width of the bin is larger than the typical error on the estimate of the magnitude. This is obviously not true since a star whose true magnitude is near the edge of a bin can migrate because of an arbitrarily small fluctuation. The effects of migration may be amplified by the completeness correction, especially in the faintest bins of the LF.

Furthermore the Completeness factor may be obtained from the artificial star experiments *only as a function of input magnitude* (say, $V_{\rm in}$) while the observed LF is (obviously) a function of the *observed magnitude*, whose corresponding quantity in the artificial star experiment is $V_{\rm out}$[6]. Thus when an observed LF is corrected by multiplying it by $1/C_f(V_{\rm in})$, it is implicitly assumed that $V_{\rm in}$ and V_{obs} are the same quantity, that, in general, is not true.

There have been few attempts to correct the observed LFs for all the effects above (Drukier et al. 1988; Stetson & Harris 1988). The proposed methods require a complex mathematical approach, and may rely on the *a priori* assumption of an analytical form of the true LF (Stetson & Harris 1988) or on approximate treatments of the propagation of errors under matrix inversions (see Drukier et al.

[4] The error associated to each magnitude entry is the error on the mean over repeated measures, see Pap I.

[5] Note that this phenomenon may significantly alter the star counts in the bins near the limiting magnitude, at least in cases in which the crowding conditions are critical, see Tosi et al. (2001), for discussion

[6] The input magnitude ($V_{\rm in}$) of artificial stars corresponds to the *true* magnitude of real stars ($V_{\rm true}$), while the output magnitude ($V_{\rm out}$) corresponds to the observed one (V_{obs}) under the extant conditions

1988; Mighell 1990, for references and discussion).

Here we propose a new method that is fully non-parametric and extremely simple in nature, taking also advantage of the huge enhancement in computational power of workstaions and PCs that took place since the times of the above quoted attempts. As we will show below (*a*) the proposed method takes full account of the effects of bin migration and (*b*) the completeness correction is consistently applied to a LF that is function of $V_{\rm in}$ as the completeness factor. The method is particularly appropriate for the application to LFs of SSPs, but it can be probably generalized to other cases. The prerequisite is the availability of huge sets of realistic artificial star experiments well sampling the whole spatial, luminosity, and color range of the observations.

3.1. *The Equivalent Sample*

Consider a large set of artificial star experiments performed in a region of uniform crowding conditions, e.g., the WF2-Ext set presented in Fig. 1. Suppose that the input magnitudes of the artificial stars be distributed as the "true" stars of the parent population (in this case the stars of NGC 288; the reasons of this hypothesis will become clear at the end ofthis section). From this set it is possible to extract a subsample of *recovered* stars with exactely the *same dimension* and the *same distribution as a function of* $V_{\rm out}$ as the observed sample. Call this subsample an *Equivalent Sample* (ES)[7]. It is important to note that the ES contains only stars that have been succesfully recovered in the artificial star experiments process, hence that have suffered only the effects of bin migration (i.e, blending and/or observational scatter).

By definition the ES has *the same output (e.g., observed) properties* of the observed sample, it is one of the many possible relizations that are mapped by the OMF from the input/true domain to the output/observed one. Thus *the input (e.g., true)* properties of the ES are one of the possible *true* set of properties that may have been mapped into the observed sample by the OMF. It is immediately apparent that the LF of the input magnitudes of the ES is equivalent to the observed LF *once corrected for all the effects of bin migration*[8]. Thus the identification of an ES allows (*a*) the removal of all the effects of bin migration and (*b*) the expression of the observed LF as a function of input magnitude, consistently with the completeness factor (see §3.). If we apply the completeness correction to the *input LF* of the ES we find one possible realization of the final LF, corrected for *all the observational effects*. Since different ES may be mapped into the same observed sample by the OMF, repeating the process for a number of (randomly extracted) different ES and taking the average will allow to obtain a final LF more robust to random fluctuations as well as a direct estimate of the uncertainty associated with the whole process.

However, there is another important factor we have to take into account. While the completeness correction is completely independent from the distribution in magnitude of the artificial star set, the derived correction for bin migration is not. Consider a given bin of the observed LF. Such a bin will be primarily filled by stars with $V_{\rm out} \simeq V_{\rm in}$, but also by a certain fraction of stars which have migrated from the nearby bins beacause of blending and photometric errors. Increasing the number of artificial stars in the nearby bins, with respect to the considered bin, will enhance the probability of extracting stars that enter in the bin because of migration, hence increasing the final "migration correction". The right correction would be obtained only if the artificial star set is distributed as the true LF of the population which is unknown, being the very target of our analysis. We circumvent this problem by iteratively adjusting (*a posteriori*) the distribution of the artificial star set until the best approximation is obtained (see below for details). The approach has proven to be successful since we obtain the same final LF *independently* of the initial distribution of the artificial star set. In the following section the adopted operational procedure is described in detail.

3.2. *Operational procedure*

For each of the four observed subsamples (PC-Int, WF-Int, PC-Ext, WF-Ext) we adopted the following procedure:

1. An initial distribution of input magnitudes is assumed for the artificial stars and the largest possible subset accordingly distributed is extracted from the whole set of artificial stars.

2. Twenty different ES are extracted at random from the above subset and their $LF(V_{\rm in})$ are corrected for completeness.

3. The (bin per bin) average of the twenty obtained LFs is adopted as the "current corrected LF" and the standard deviation is adopted as the corresponding uncertainty.

4. The "current corrected LF" is assumed as the distribution of the artificial stars and a new subset of artificial stars accordingly distributed is extracted from the whole set of artificial stars as in step 1.

5. The steps 2,3 and 4 are repeated twenty times. The twentieth "current corrected LF" is adopted as the *final LF* with the corresponding uncertainties.

Step 4 ensures that at each new iteration the adopted set of artificial stars will become more and more similar to the "true" one, giving increasingly appropriate rates of bin migration.

In all the cases considered here the process converged in ≤ 6 iterations, e.g., the "current corrected LFs" become very stable after the sixth iteration. Furthermore, the result is independent of the initial distribution of input magnitudes that is assumed for the artificial star subset. We have tried many different distributions (some of which are

[7] The operational procedure to extract an ES is the following. Consider the histogram representing the *observed* LF: each bin i contains N_i stars. From the artificial star set we extract at random N_i stars whose *output* magnitudes lie in the i-th bin. Repeating this step for each bin of the observed LF we obtain a sample of recovered artificial star that have an *output* LF equal to the *observed* one. Note that the same procedure can be applied on a star-by-star basis, by randomly extracting an *artificial sister* (see §3.4) for each *observed* star.

[8] In other words the LF of the input magnitudes of the ES is the observed LF seen *before* any blending and/or observational error take place.

shown in Fig. 2) and in all cases the process converged to *the same final LF* in few iterations.

Some examples of the procedure are shown in Fig. 2, applyied to the WF-Ext sample. In Fig. 2a the artificial star subset was initially distributed as the observed LF down to $V \leq 25.5$ and uniformly from this limit down to $V = 27$. A scaled version of the adopted distribution is plotted as a thick dotted line. The thin dotted histogram shows the "current corrected LF" after the first iteration of the process, the thin continuous histogram shows the "current corrected LF" after the sixth iteration and the open dots are the final LF, corresponding to the twentieth iteration of the process, with the currrent standard deviation of the twenty realizations of the corrected LFs as errorbars. The encircled dot is the first bin of the LF for which $C_f < 0.5$, i.e. the completeness correction is larger than a factor 2. The fast convergence and the stability of the final solution can be readily appreciated.

Fig. 2b and 2c have the same symbols of Fig. 2a but shows the convergence of the process starting from (very) different initial distributions of the artificial star subset. The open dots are *the same final LF shown in Fig. 2a.* Thus Fig. 2a and 2b shows that the process converges to *the same final LF* independently of the assumed initial distributions of the artificial stars subset.

Finally, Fig. 2d shows in detail the results of the twentieth (i.e. final) iteration of the process shown in Fig. 2a. The twenty histograms are the corrected LFs obtained by the twenty different ES extracted from the finally adopted subset of artificial stars. The full dots and errorbars are their means and standard deviations.

3.2.1. *The final LFs*

Since the obtained LFs are independent from the initial distribution of the adopted subset of artificial stars, we derived our final (corrected) LFs for all the considered samples assuming the same initial distribution of the artificial stars shown in Fig. 2a. The final LFs are given in Table 1 (PC-Int and WF-Int samples) and in Table 2 (PC-Ext and WF-Ext samples). The table gives the $V_{\rm in}$ (e.g., $V_{\rm true}$) of the center of the bins and, for each sample, the observed LF, the completeness factor C_f, the final LF and the total error on the final LF (see below).

The final LF is given down to the first bin that has $C_f < 0.50$. In the following plots this point is circled to serve as a reminder that it is has been derived applying a large correction. We retain these points as educated guesses of the behaviour of the LFs beyond the range in which moderate and safe corrections can be made. We consider as fully reliable only the points of the LF for which $C_f \geq 0.50$. We note that the last fully reliable points, according to the above criterium, have $C_f = 0.607, 0.769, 0.806, 0.842$ for the PC-Int, WF-Int, PC-Ext, and WF-Ext samples, respectively. Thus the completeness is quite high for the whole considered range.

The final total error reported in Tab. 1 and 2 has been obtained by summing in quadrature the error on the Completeness factor (**?**, estimated according to Eq. 18 by)]ken, to the standard deviation of the twenty different realizations of the LF that are obtained in the last step of the procedure (see §3.2 and Fig. 2d). In all the following plots the errorbars associated with the LFs of NGC 288 represent this final total error.

The final LFs (open dots) are shown with the corresponding observed LF (full dots) in Fig. 3.

As a further check we compared our final LFs with those obtained by dividing the observed $LF(V_{obs})$ by $C_f(V_{\rm in})$. We note that the differences are within 1σ in most bins and $< 2\sigma$ in any bin. As expected, in this particular application the effects of bin migration are not large. This would not be the case if much more crowded fields were considered (**?**, see §3. and)]tosi.

3.3. *The effect of binary systems on the LF*

There is an intrinsic kind of blending that cannot be directly tackled with artificial star experiments. Physical binary systems are strictly equivalent to chance superposition blendings. The LF for *single stars* cannot be obtained if an independent estimate of the incidence of binary systems is not available. Further, since the actual binary fraction (f_b) depends on the (unknown) distribution of mass ratios ($F(q)$; see Pap I), any correction would be model dependent. Indeed, a direct estimate of the impact of binary systems on the LF of a globular cluster has only been possible for NGC 6752 (Rubenstein & Bailyn 1999).

Now we can add a second cluster using the results of Pap I. We measured f_b in the Int and Ext regions of NGC 288. In the Int region we found that the observations are compatible with $8\% \leq f_b \leq 38\%$, and the most probable range is $10\% \leq f_b \leq 20\%$. In the Ext region $f_b \leq 10$ % and the most probable value of f_b is zero, independently of the assumed $F(q)$. Thus, a sizeable fraction of binary systems is present in NGC 288, at least in the Int sample, and may affect the derived LF of single stars.

To quantify the effect we computed the mean bin-by-bin ratio between the LFs obtained by 5 ES with $f_b = 20$ % and by 5 ES with $f_b = 0$ %. This number gives (approximately) the fractional variation of the star content of the bins due to binary systems. Furthermore, dividing the final LF by the quoted ratio, the LF is corrected for the binary content and mapped to the "pure single stars" case. In Fig. 4 the final LF of the WF-Int sample not corrected for the binary content (filled dots with error bars) is compared with its binary-corrected versions in the assumption $f_b = 20$ % and for three different $F(q)$ (see caption and Pap I for details). The comparison is performed in the magnitude range in which the binary estimate of Pap I has been performed ($20 \leq V \leq 23.5$).

There are several noteworthy features in Fig. 4: 1) The maximum correction is $\leq 3\%$. 2) All the corrected LFs lie within the uncertainties of the un-corrected one. 3) The PLMR $F(q)$ case is most similar to the uncorrected case. This was expected, since in this case the large majority of binary system has a very low mass secondary. This means that the migration of the primary is small, and that most of the secondary stars are so faint that they fall in an unobserved region of the LF. 4) The correction for the PHMR case depletes the intermediate bins ($21.5 \leq V \leq 23$; because it corrects for the migration of primary) and enhances the last bin because of the recovery of some secondary stars as single stars. 5) No bin is exclusively depleted or enhanced by the redistribution of the binary components as single stars.

From the above results and discussion we conclude that:

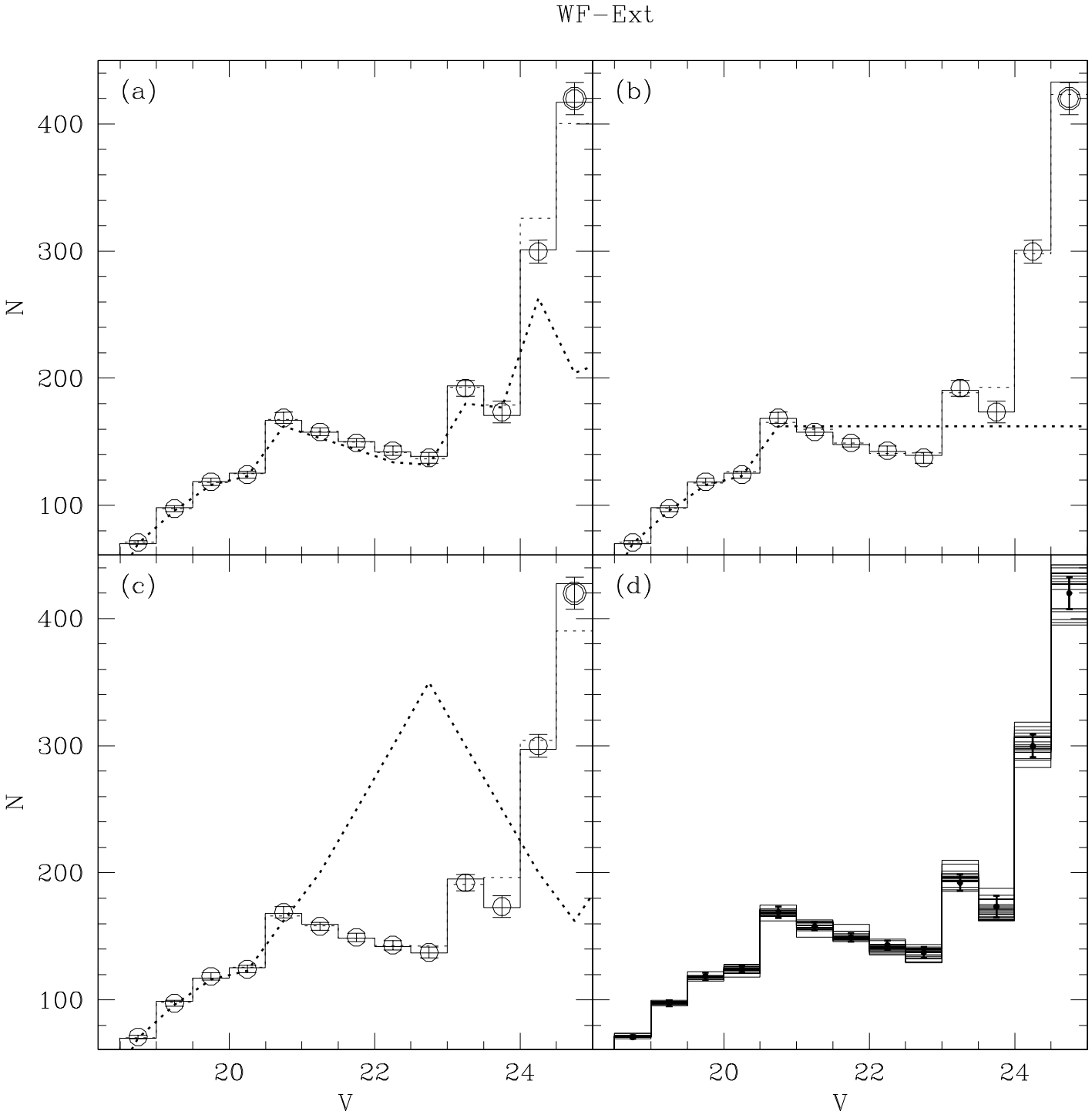

FIG. 2.— Panel (a): The final LF is shown as open dots with error bars (the same LF is reported with the same symbols also in panels *b* and *c*). The encircled dot is the first point with $C_f < 50$ %. The thick dotted line is a scaled version of the distribution of $V_{\rm in}$ of the artificial stars subsample adopted for the first iteration, in the present case assumed with the same shape of the *observed* LF to $V = 25$ and with $N = 215$ for the $V > 25$ bins (in the present scale). The thin dotted histogram is the LF recovered after the *first* iteration of the process. The thin continuous histogram is the LF recovered after the *sixth* iteration, when convergence has been reached. Panel (b): the same as Panel (a) but adopting a different distribution for the artificial stars subsample adopted for the first iteration (i.e., flat for $V \geq 20.5$). Panel (c): the same as panels (a) and (b) for an initial distribution for the artificial stars subsample strongly peaked at $V = 22.75$. Panel (d): the twenty realizations of the last iteration of the process for the case shown in Panel (a). The final LF is the mean of the twenty realizations (full dots) and the uncertainty associated with the process is the corresponding standard deviation.

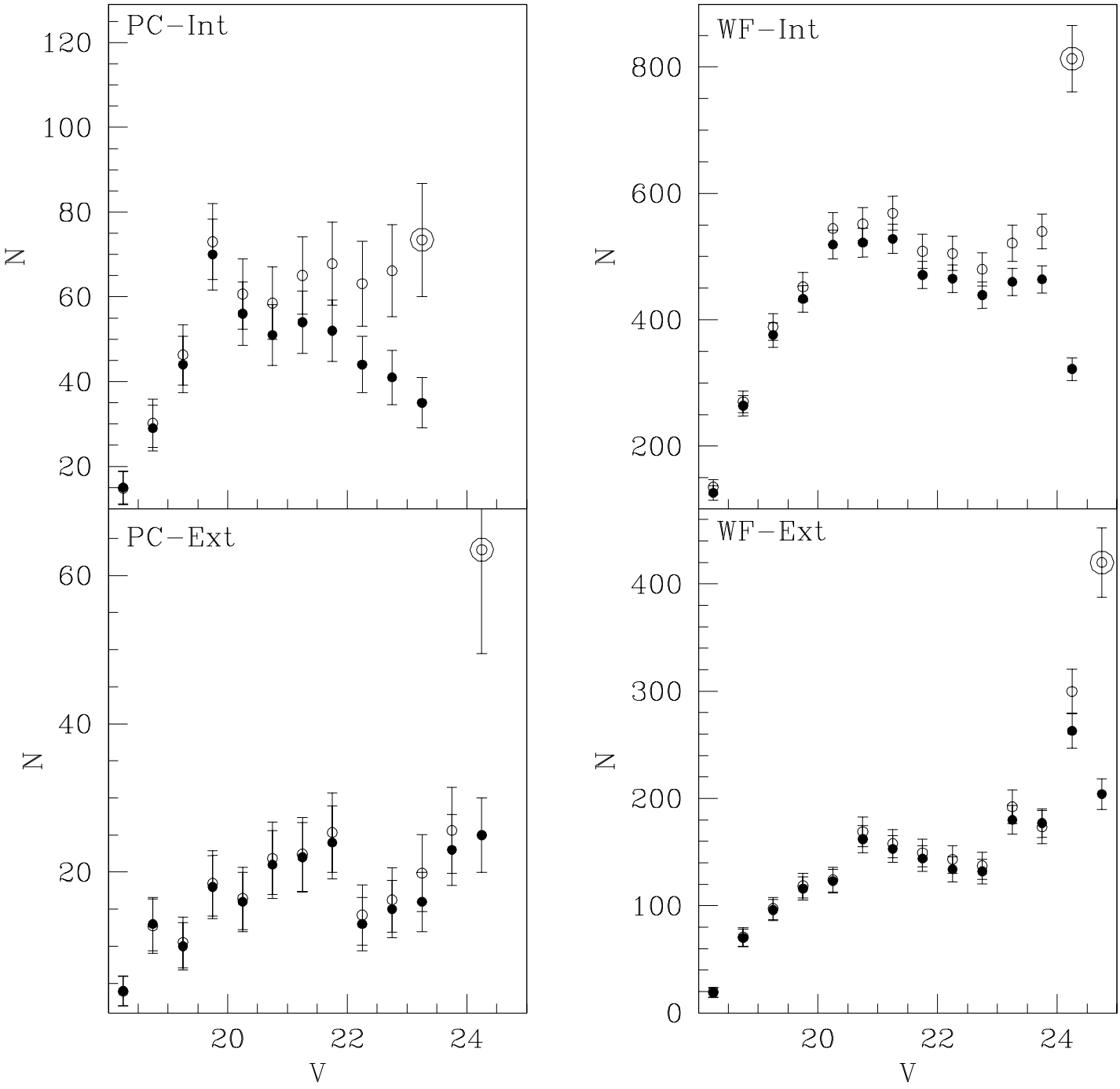

FIG. 3.— The observed (filled circles) and corrected LFs of the four samples. The encircled point is the first bin for which $C_f < 0.50$.

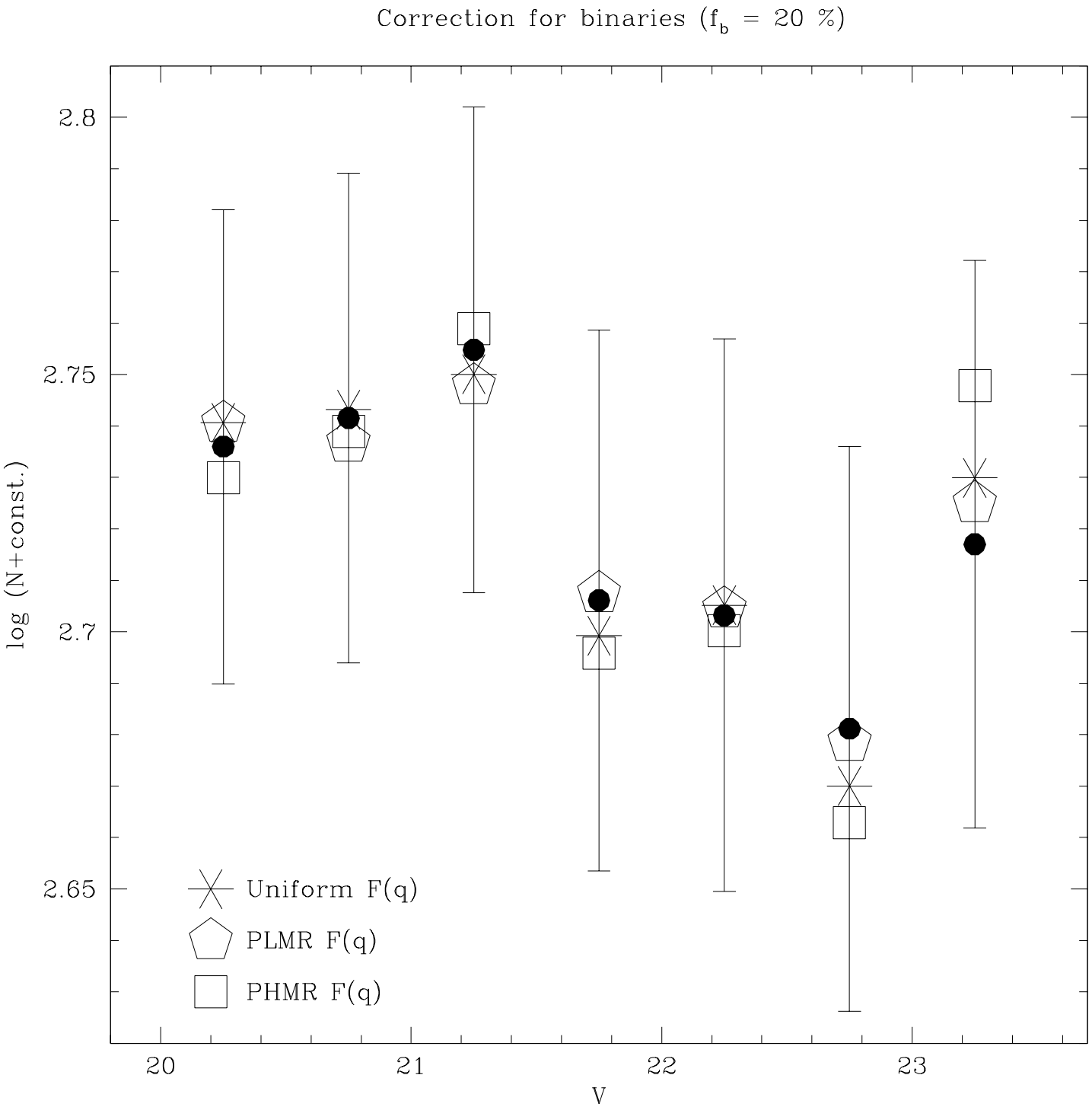

FIG. 4.— The final LF of the WF-Int sample without correction for binary systems (full dots with errorbars) is compared with the same LF after a correction for a binary fraction $f_b = 20\%$, under different assumption on the mass ratios ditribution ($F(q)$). Open squares: PHMR (peaked at high mass ratios) $F(q)$; stars: Uniform (all mass ratios are equally probable) $F(q)$; open pentagons: PLMR (peaked at low mass ratios) $F(q)$. The corrected LFs are very similar to the uncorrected one, thus the correction for binary system can be neglected in the present case.

1. The correction for binary systems can be safely neglected for the Ext samples where the binary fraction is much lower than $f_b = 20$ % and possibly null.

2. The correction can be neglected also for the Int samples, at least for $V < 23.5$, since it is smaller than the uncertainties of the final LF. However, it cannot be excluded that the faintest bins of the single stars LF need a significant enhancement to take into account the effect of binaries, particularly if the actual $F(q)$ favors high mass ratios.

3.4. *Further developements and other applications*

The case under study is particularly simple. NGC 288 is a very loose and relatively nearby cluster, so our WFPC2 observations well resolve the large majority of the stars down to the limiting magnitude of each subsample with a very high degree of completeness. Further, the density gradient is a very fortuitous match to WFPC2 allowing a few large subsamples to nicely probe radial variations.

It is important to note that the Equivalent Sample concept does not require such simplifications and may be successfully applied under any condition. If a strictly rigorous approach is adopted the ES approach may have far reaching applications in the study of stellar populations. Here we provide two possible examples to show the potential of the method.

- **Extremely crowded field with strong density gradient**. The method can tackle with samples with arbitrarily large density gradient, for instance by subdividing the observed sample in subsamples whith nearly uniform stellar density (as done in the present application). If the dimension of the observed sample is not sufficiently large to allow this approach, the ES method can be implemented also on a star-by-star basis. It will suffice to assemble the ESs by associating an artificial star analogue for *each* observed star, randomly extracted from a set of artificial stars having (approximately) the same $V_{\rm out}$ and position in the frame of the considered observed star (*artificial sisters*). The only basic requirement to successfully follow this approach is to have a very large set of artificial stars, sampling with large multiplicity the whole range of magnitudes and positions covered by the observed sample.

- **Mapping synthetic CMDs into the observational plane**. The standard tool used to derive the Star Formation History (SFH) from the CMD of a resolved galaxy consist in the reproduction of observed CMD by a synthethic CMD in which the stars are extracted from theoretical evolutionary tracks (see Lejeune et al. 2001, for references and discussion of the various adopted techniques). To transform the synthetic CMD to the observational plane the effects of incompleteness, blending and observational scatter must be added to the synthetic stars. This task is not easy and it is usually done with simplified approaches. For instance, the observational scatter is usually introduced by randomly extracting 'errors' from gaussian distributions with standard deviations equal to the typical 1σ photometric error. However, the distribution of the observational scatter is not gaussian, in general, and it is not easy to parametrize. Furthermore, the effects of blending are not separable from the effects of observational scatter, and gaussian distributions do not provide a good reproduction of the real distribution, introducing undesired noise in the comparisons.

  With the ES approach, one can easily map the *input magnitudes* (e.g., "true" magnitudes) extracted by the evolutionary track in to the observational plane with the correct OMF, by "asking" to the artificial stars experiments what is the probabilty that such star would be successfully recovered or not. If a star passes the "incompleteness barrier", it can be correctely mapped into the observational plane, for instance by assigning to it the output properties of an artificial analog extracted at random from a set of *artificial sisters*.

  In this way, the whole effects of the OMF would be correctly reproduced without dangerous approximations and/or parametrizations.

4. COMPARISON OF LFS

Once the observed LFs have been corrected for all the observational effects and the impact of binary systems have been quantified, we can use the final LF to study the dynamical status of NGC 288 either comparing the LFs in the Int and Ext regions of the cluster, either comparing the LF of NGC 288 with those of other clusters. In the following we will normalize all the samples to be compared to the number of stars in the range $18.5 \leq V \leq 20.5$, following the approach of **?**)][hereafter PZ99]manu99.

NGC 288 is not sufficiently nearby to allow a safe derivation of the LF down to the hydrogen burning limit even with HST. The comparison with other "state of the art" LFs of more nearby clusters (see Fig. 6, below) shows that such limit would occur a couple of magnitudes below our faintest valid point (the faintest bin of the WF-Ext LF). The Mass-Luminosity relation adopted in Pap I indicates that the lowest mass efficiently sampled by our deepest LF is $M \simeq 0.35\,M_{\odot}$. Usually MF are compared according to their slope in the plane $\log N - \log M$ for $M \leq 0.5\,M_{\odot}$ (see PZ99 and references therein). Our best LF has just three points below this limit, thus the slope of the MF would be poorly constrained. Because of this limitation we avoid any conversion of our LFs to Mass Functions (MF), since that would necessarily be somewhat model dependent and uncertain (see, e.g., Bedin et al. 2001). Instead we will make direct comparisons between LFs in the allowed range.

4.1. *Mass segregation within single stars in NGC 288*

The LFs of the PC fields are identical (to within the errors) to those of the respective WF samples, in the range where the comparison is possible. Since the WF samples are much larger and reach fainter magnitudes we will limit our analysis to these homogeneous datasets in the following.

In Fig. 5 the LFs from the WF-Int and the WF-Ext samples are compared. It is evident at a first glance that the

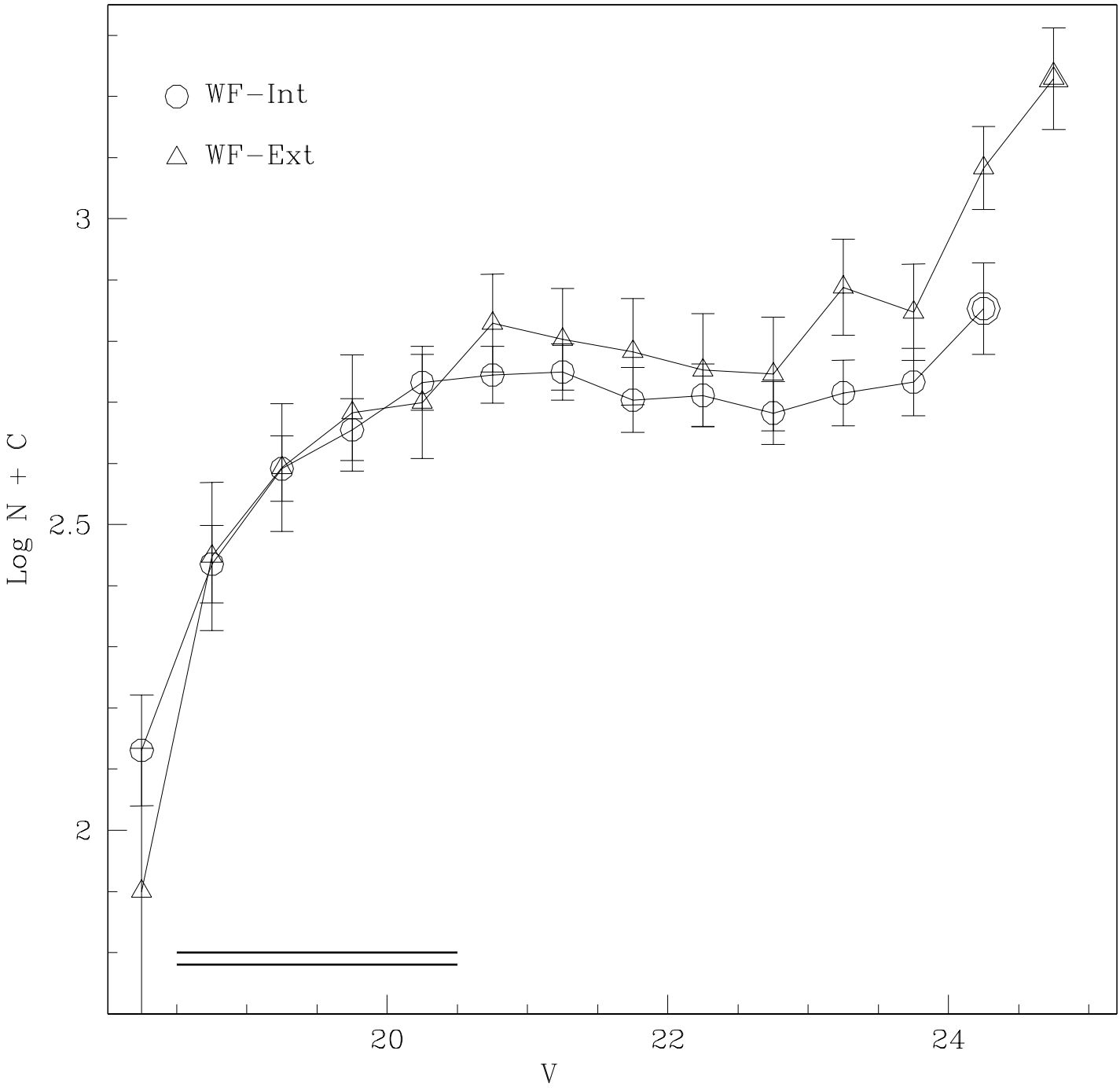

FIG. 5.— Comparison between the LFs of the WF-Int sample (open circles) and of the WF-Ext sample (open triangles). The encircled points are the first points with $C_f < 0.50$.The horizontal bars indicate the normalization interval.

LF of the WF-Int sample is flatter than that of WF-Ext. Given the adopted normalization, this is a clear indication of a depletion of low mass stars in the region within $1\,r_h$ (Int) with respect to the Ext field. If the brightest bin is included in the normalization the effect is significantly enhanced. We note also that any correction for binaries would be much smaller than the observed difference (see Fig. 4). On the other hand, if fainter stars ($20.5 < V \leq 24$) are used for normalization, one would infer a substantial excess of the more massive stars in the Int sample.

Independently of the assumed normalization it is worth establishing if the difference between the two LFs is statistically significant. To check this hypothesis we performed a χ^2 test, adopting the appropriate definition of the statistic according to Eq. 14.3.3 by Press et al. (1992). The comparison has been performed in the safely comparable range $18.5 \leq V \leq 24$. The resulting reduced χ^2 is 2.31 with 12 degrees of freedom. The difference between the two LFs is found to be significant at the 99.1 % confidence level, i.e. *highly significant*.

We have already demonstrated that mass segregation exists in NGC 288, since both binary systems and their by-product Blue Stragglers Stars are also more centrally concentrated than the the single stars. Although the evidence is not as strong (because of the possible ambiguity in the interpretation associated with the choice of the normalization range), we feel that we now find some evidence for further mass segregation in the difference between the LFs of unevolved stars in the Int and Ext regions of the cluster.

4.2. *Low mass star depletion in NGC 288*

In Fig. 6 the WF-Int and the WF-Ext LFs of NGC 288 are compared with the LFs of M10, M22 and M55 by PZ99. The transformation from apparent to absolute magnitude has been obtained by assuming $(m - M)_0 = 14.67$ and $E(B - V) = 0.03$, according to Ferraro et al. (1999). The faintest point of the WF-Ext LF reaches $M_V \simeq 10$ while the LF of the (more nearby) PZ99 clusters reaches $M_V \simeq 12$–13. The faintest reported point appear to coincide with the turn-over point found in the LFs of the PZ99 clusters, so this possible feature in the LF of NGC 288 is not detectable in our data (but it have been apparently detected by Pasquali, Brigas & De Marchi 2000, hereafter PBD00).

On the other hand, the comparison in the range $6 < M_V \leq 10$ shows that the LF of NGC 288 is significantly flatter than those of M10, M22 and M55. Note that the LFs of these clusters were obtained near the half-mass radius (usually approximated with the half light radius r_h, see Djorgovski 1993). This is the region where the mass distribution of the cluster population is expected to be fairly representative of the (present day) global population (see Meylan & Heggie 1997; Vesperini & Heggie 1997, and references therein). Since the Int and Ext sample are separated at $1\ r_h$, the LF at the half-mass radius must be intermediate between the WF-Int and the WF-Ext, and the derived LFs should be representative of the global LF of NGC 288.

The comparison presented in Fig. 6 strongly suggests that the global population of NGC 288 is significantly depleted of low mass stars with respect to M10, M22 and M55 (see PZ99 for an indirect comparison with other clusters).

NGC 288 has a mass ranging from $\sim \frac{1}{2}$ to $\sim \frac{1}{6}$ that of the comparison clusters. Its central density ranges from $\sim \frac{1}{2}$ to $\sim \frac{1}{60}$ (Pryor & Meylan 1993) that of the comparison clusters. Thus NGC 288 is intrinsically less resistent to harrassment and heating by external forces. Furthemore, among the clusters considered here, it moves on the orbit having the smallest perigalactic distance, the highest eccentricity and the highest inclination to the Galactic plane. Hence, it is expected to suffer strong bulge and disk shocks, and indeed may be one of the clusters with the highest disruption rates (Dinescu, Girard & van Altena 1999; Gnedin & Ostriker 1997). The coupled effects of internal energy equipartition (mass segregation), pushing the lighter stars to outer, shallowly bound orbits, and of the tidal field of the Galaxy, removing the less bound stars venturing in the outer parts of the cluster halo, may well be at the origin of the depletion of lighter stars in NGC 288. We regard this result as a reassuring confirmation of the theoretical predictions that account for the orbital characteristics of actual GGCs (Dinescu, Girard & van Altena 1999; Gnedin & Ostriker 1997).

Recently, PBD00 presented a LF in the J and H near-infrared bands obtained with the HST NIC3-NICMOS camera (parallel observations). The sample is small but reachs fainter magnitudes (lighter masses) than our data. PBD00 conclude that the mass function of NGC 288 is very similar to that of all other studied clusters, and that it shows no sign of the strong harrassment predicted by Dinescu, Girard & van Altena (1999) and Gnedin & Ostriker (1997). We regard the results (and the conclusions) of the present paper as more robust than those by PBD00 since: *(a)* the LF by PBD00 is based on a sample of 75 stars, a very small sample that may be subject to strong statistical fluctuations, and is not supported by artificial star experiments, while our LF is based on a sample of more than $6,000$ stars corrected for all the observational biases with the artificial star experiments; and *(b)* the field observed by PBD00 is a small stamp ($51\farcs2 \times 51\farcs2$, ~ 15 times smaller than the field observed here) located at $r \sim 2.4\,r_h$, far outside the region of our sample which is expected to be representative of the global cluster LF.

5. SUMMARY AND CONCLUSIONS

The LF of the globular cluster NGC 288 (down to $M_V \sim 10$) has been obtained from a field covering a region comprised between the center of the cluster and $r \sim 2\,r_h$.

A new method to correct the observed LFs for all the observational effects have been introduced and applied. The method is based on the Equivalent Sample concept, which may have many interesting applications in the study of stellar populations.

The effect of the presence of binary systems in the final LF has been quantified and it has been found negligible, in the considered magnitude range.

Comparison of the LFs obtained in different regions of the clusters, indicates the presence of mass segregation within NGC 288. Independently of the assumed normalization the LFs of the inner (WF-Int) and outer (WF-Ext) sample turns out to be different at the 99.1 % confidence level.

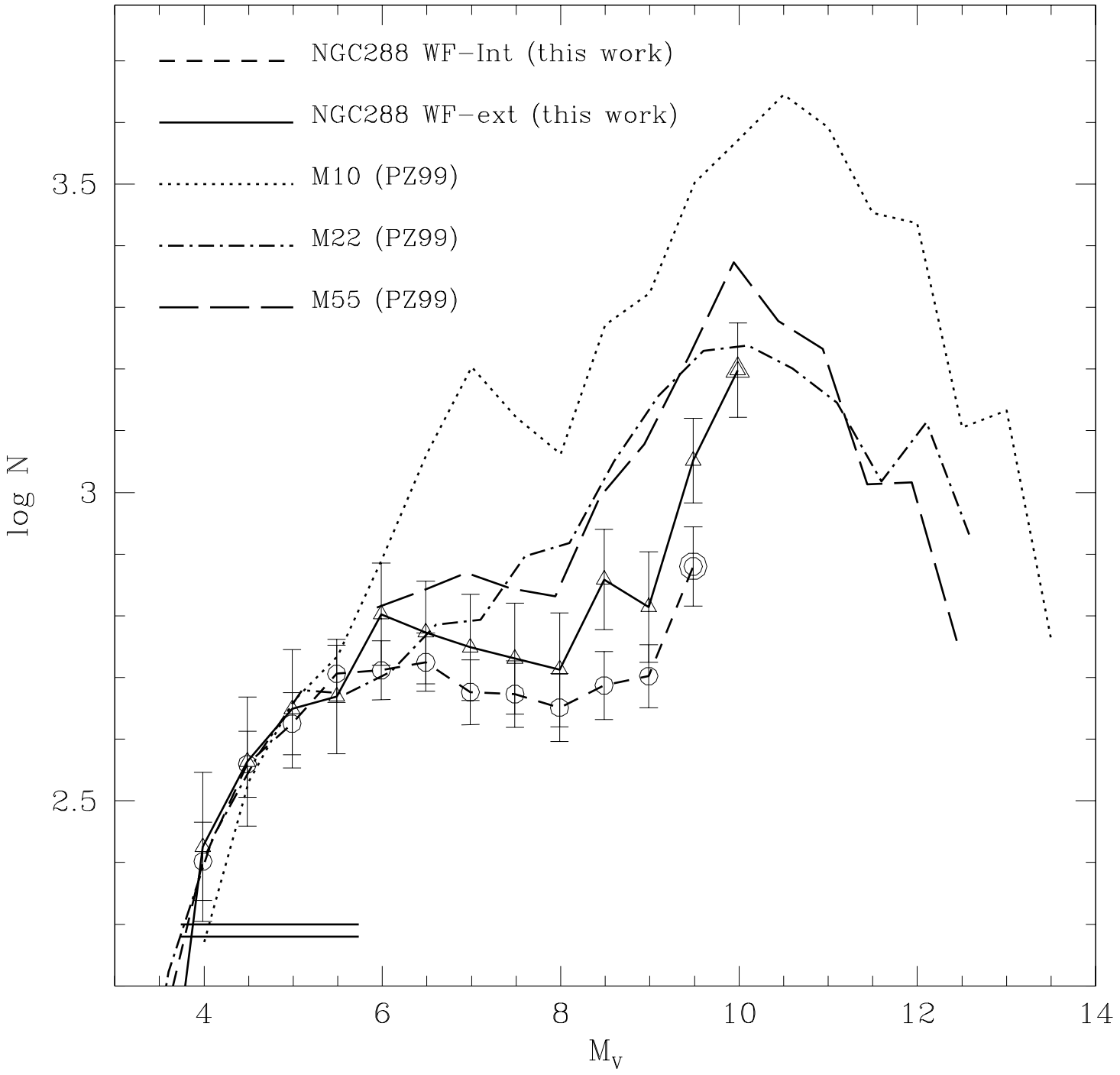

FIG. 6.— Comparison between the WF-Int and Wf-Ext LFs of NGC 288 with the LFs of M10, M22 and M55 by PZ99. The encircled points are the first points with $C_f < 0.50$. The horizontal bars indicate the normalization interval.

The comparison with the LFs of other clusters strongly suggests that the global population of unevolved stars in NGC 288 is significantly depleted of low mass stars ($M \leq 0.5$–$0.6\,M_{\odot}$), in general agreement with the predictions of recent theoretical predictions taking into account also the orbital properties of the cluster.

The financial support of the *Agenzia Spaziale Italiana* (ASI) is kindly acknowledged. The financial support to M. Messineo has been provided by the Osservatorio Astronomico di Bologna. Part of this work has been the subject of the Thesis of Degree of L. Monaco (Dept. of Astronomy, Bologna University). Part of the data analysis has been performed using software developed by P. Montegriffo at the Osservatorio Astronomico di Bologna. RTR is partially supported by NASA LTSA Grant NAG 5-6403 and STScI grant GO-8709. This research has made use of NASA's Astrophysics Data System Abstract Service.

REFERENCES

Andreuzzi, G., De Marchi, G., Ferraro, F.R., Paresce, F., Pulone, L., Buonanno, R. 2001, A&A, 372, 851
Bedin, L.R., Anderson, J., King, I.R., & Piotto, G. 2001, ApJ, 560, L75
Bellazzini, M., Ferraro, F.R., Fusi Pecci, F., Galleti, S., Catelan, M., Landsman, W.B. 2001a, AJ, 122, 2569
Bellazzini, M., Fusi Pecci, F., Messineo, M., Monaco, L., Rood, R.T. 2001b, AJ, in press (Pap I)
Catelan, M., Bellazzini, M., Landsman, W.B., Ferraro, F.R., Fusi Pecci, F., Galleti, S. 2001, AJ, 122, 3171
Djorgovski, S.G. 1993, in Structure and Dynamics of Globular Clusters, S.G. Djorgovski and G. Meylan eds., ASP, S. Francisco, ASP Conf. Ser., vol. 50, p. 373
Dinescu, D.I., Girard, T.M., van Altena, W.F. 1999, AJ, 117, 1792
Drukier, G.A., Fahlman, G.G., Richer, H.B., & VandenBerg, D.A., 1988, AJ, 95,1415
Harris, W.E. 1996, AJ, 112, 1487
King, I.R., Anderson, J., Cool, A., Piotto, G. 1998, ApJ, 492, L37
Lejeune, T., & Fernandes (eds.), J., 2001, Observed HR diagrams and stellar evolution: the interplay between observational constraints and theory, ASP, S. Francisco, ASP Conf. Ser., in press
Marconi, G., Buonanno, R., Carretta, E., Ferraro, F.R., Montegriffo, P., Fusi Pecci, F., De Marchi, G., Paresce, F., Laget, M. 1998, MNRAS, 293, 479
Gnedin, O., Ostriker, J.P. 1997, ApJ, 474, 223
Meylan, G., & Heggie, D. C. 1997, A&A Rev., 8, 1
Mighell, K.J. 1990, A&AS, 82, 207
Ferraro, F.R., Carretta, E., Bragaglia, A., Renzini, A. Ortolani, S. 1997, MNRAS, 286, 1012
Ferraro, F.R., Messineo, M., Fusi Pecci, F., Straniero, O., Chieffi, A., & Limongi, M. 1999a, AJ, 118, 1758
Pasquali, A., Brigas, M.S., De Marchi, G. 2000, A&A, 362, 557 (PBD00)
Paresce, F., De Marchi, G. 2000, ApJ, 534, 870
Piotto, G., & Zoccali, M. 1999, A&A, 345, 485 (PZ99)
Piotto, G., & Zoccali, M. 2000, A&A, 358, 943 (PZ00)
Press, W.H., Teukolsky, S.A., Vetterling, W.T., & Flannery, B.P., 1992, Numerical recipes (2nd edition), Cambridge, Cambridge University Press
Pryor, C., Meylan, G. 1993, in Structure and Dynamics of Globular Clusters, S.G. Djorgovski and G. Meylan eds., ASP, S. Francisco, ASP Conf. Ser., vol. 50, p. 357
Rosenberg, A., Saviane, I., Piotto, G., & Aparicio, A. 1999, AJ, 118, 2306
Rosenberg, A., Piotto, G., Saviane, I., & Aparicio, A. 2000, A&AS, 144, 5
Rubenstein, E. P., & Bailyn, C. D., 1997, ApJ, 474, 701 (RB97)
Rubenstein, E. P., & Bailyn, C. D., 1999, ApJ, 513, L33 (RB99)
Shetrone, M. D., & Keane, M. J. 2000, AJ, 119, 840
Stetson, P.B., & Harris, W.E., 1988, AJ, 96, 909
Tosi, M., Sabbi, E., Bellazzini, M., Aloisi, A., Greggio, L., Leitherer, C., Montegriffo, P., AJ, 122, 1271
Vesperini, E., Heggie, D.C. 1997, MNRAS, 289, 898

TABLE 1
PC-INT AND WF-INT LUMINOSITY FUNCTIONS

	PC-Int				WF-Int			
V	$N_{\rm obs}$	C_f	N_c	σ_{Nc}	$N_{\rm obs}$	C_f	N_c	σ_{Nc}
18.25	15	0.978	14.8	3.9	126	0.956	135.1	12.2
18.75	29	0.963	30.2	5.7	264	0.981	270.2	17.1
19.25	44	0.957	46.3	7.1	376	0.975	388.6	20.8
19.75	70	0.946	73.0	8.9	433	0.972	452.1	22.8
20.25	56	0.920	60.7	8.3	519	0.969	544.5	25.1
20.75	51	0.898	58.5	8.5	522	0.956	551.5	26.2
21.25	54	0.832	65.1	9.1	528	0.947	568.6	26.9
21.75	52	0.767	67.8	9.8	471	0.935	508.3	26.7
22.25	44	0.695	63.1	10.0	465	0.927	504.9	27.1
22.75	41	0.607	66.2	10.9	439	0.913	479.9	26.3
23.25	35	0.490	73.4	13.3	460	0.899	521.2	28.8
23.75	31	0.203	···	···	464	0.796	539.6	27.5
24.25	2	0.016	···	···	322	0.410	813.1	52.3
24.75	0	0.000	···	···	75	0.096	···	···
25.25	0	0.000	···	···	8	0.011	···	···

Note. — The V columns reports the $V_{\rm in}$ ($V_{\rm true}$) magnitude of the center of the 0.5 mag bins. $N_{\rm obs}$ is the observed number of stars in the bin. C_f is the completeness factor in the center of the bin. N_c is the corrected number of stars in the bin (i.e. this column contains the final corrected LF) and σ_{Nc} is the error on N_c. The final corrected LFs are reported only down to the first bin with $C_f < 50\%$.

TABLE 2
PC-EXT AND WF-EXT LUMINOSITY FUNCTIONS

	PC-Ext				WF-Ext			
V	$N_{\rm obs}$	C_f	N_c	σ_{Nc}	$N_{\rm obs}$	C_f	N_c	σ_{Nc}
18.25	4	0.996	3.9	2.0	19	0.945	19.4	4.5
18.75	13	0.989	12.7	3.6	70	0.991	70.8	8.6
19.25	10	0.987	10.5	3.4	96	0.984	97.4	10.2
19.75	18	0.980	18.5	4.4	116	0.982	118.6	11.4
20.25	16	0.980	16.4	4.2	123	0.983	124.2	11.6
20.75	21	0.980	21.8	4.9	162	0.975	168.9	14.0
21.25	22	0.964	22.4	5.0	153	0.971	157.8	13.1
21.75	24	0.947	25.3	5.3	144	0.961	149.2	12.8
22.25	13	0.915	14.2	4.1	134	0.954	143.1	12.9
22.75	15	0.895	16.3	4.3	132	0.953	137.3	12.7
23.25	16	0.879	19.9	5.2	180	0.943	192.2	15.6
23.75	23	0.806	25.6	5.8	177	0.938	173.4	15.5
24.25	25	0.369	63.5	14.0	263	0.842	299.7	20.5
24.75	5	0.069	···	···	204	0.466	419.9	32.2
25.25	0	0.004	···	···	51	0.116	···	···

Note. — The V columns reports the $V_{\rm in}$ ($V_{\rm true}$) magnitude of the center of the 0.5 mag bins. $N_{\rm obs}$ are the observed number of stars in the bin. C_f is the completeness factor in the center of the bin. N_c is the corrected number of stars in the bin (i.e. this column contains the final corrected LF) and σ_{Nc} is the error on N_c. The final corrected LFs are reported only down to the first bin with $C_f < 50\%$.

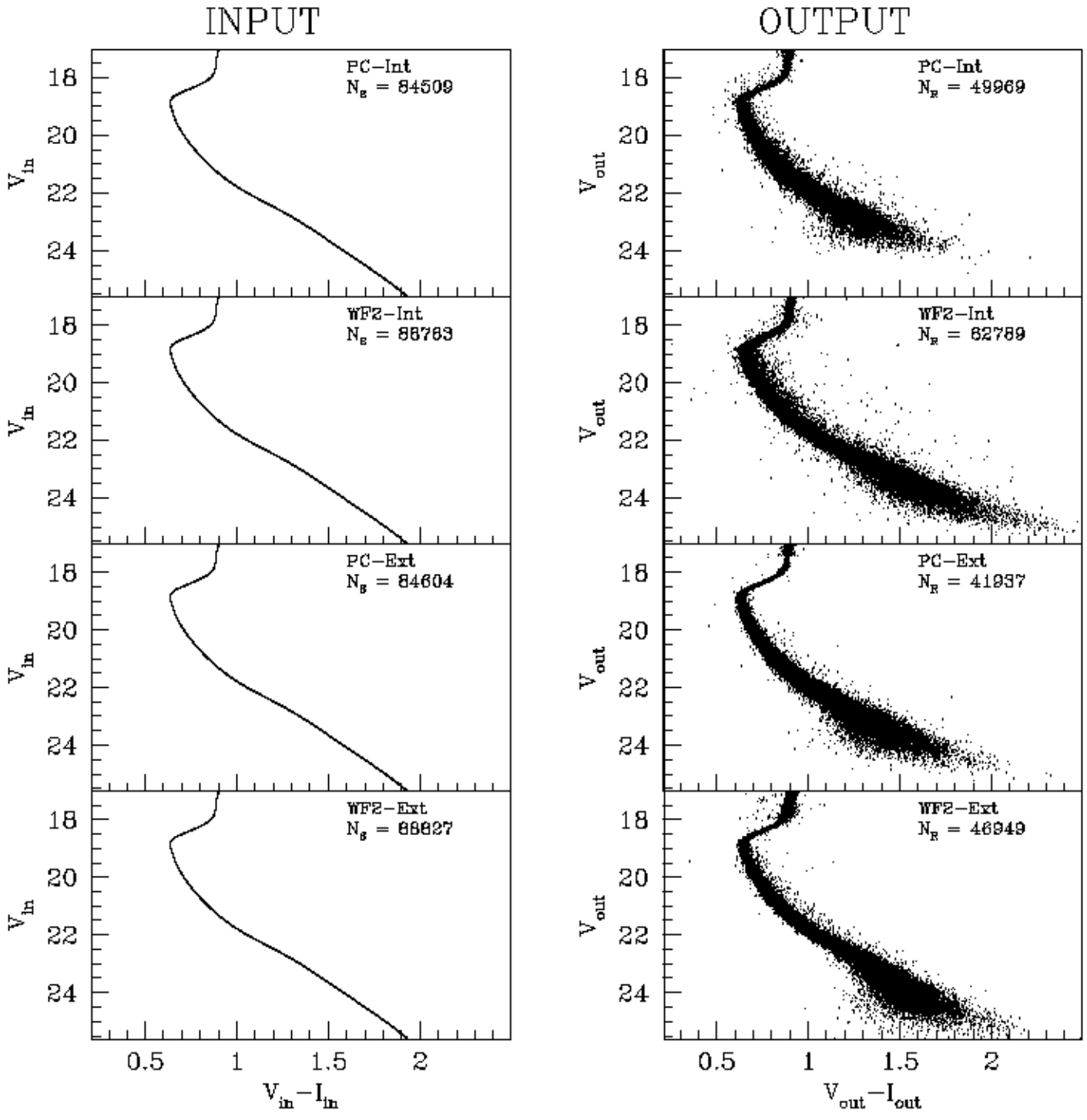
INPUT
OUTPUT
PC–Int
N_S = 84509
WF2–Int
N_S = 88763
PC–Ext
N_S = 84604
WF2–Ext
N_S = 88827
PC–Int
N_R = 49969
WF2–Int
N_R = 62789
PC–Ext
N_R = 41937
WF2–Ext
N_R = 46949
V_in
V_out
V_in − I_in
V_out − I_out
18
20
22
24
0.5
1
1.5
2